Engineering Science and Technology, an International Journal 40 (2023) 101362

HOSTED BY

ELSEVIER

Contents lists available at ScienceDirect

Engineering Science and Technology, an International Journal

journal homepage: www.elsevier.com/locate/jestch

Solar thermal waste heat energy recovery in solar distillation systems by using thermoelectric generators

Yasin Özcan [a,*], Emrah Deniz [b]

[a] Kastamonu University, Mechanical Engineering Department, Kastamonu, Türkiye
[b] Karabuk University, Mechanical Engineering Department, Karabuk, Türkiye

ARTICLE INFO

Article history:
Received 27 September 2022
Revised 24 December 2022
Accepted 7 February 2023
Available online 24 February 2023

Keywords:
Solar desalination
4E analysis
Thermoelectric
Productivity
CO_2 emissions

ABSTRACT

In this study, the novel use of thermoelectric technology in solar desalination systems was experimentally investigated. The new type of solar still with the thermoelectric generator (CSS-TEG) was proposed to improve the water output and efficiency. CSS-TEG's performance was assessed and compared with the conventional one (CSS). Economic and enviro-economic assessments, as well as energy and exergy analyses, were conducted based on the system parameters and measurements taken from the designed experimental setup. The new system's daily energy and exergy efficiency were obtained as 40.34% and 2.462% respectively, whereas, with the CSS one, they were 35.55% and 2.403%, respectively. The daily production of distilled water from the CSS and the newly designed solar still with TEG was measured at 4313 g/m^2 and 4893 g/m^2, respectively. In general, the estimated production cost of 1 kg of freshwater from CSS was 0.055$, and CSS-TEG was 0.081$. Additionally, referring to the exergo-economic parameter, CSS and CSS-TEG mitigated an average of 0.596 and 0.6132 tons of CO_2 respectively.

1. Introduction

Being vital for life, freshwater resources are under threat of overpopulation and increased industrialization along with water pollution. Scarce resources of fresh water can also trigger a global food crisis, as the agriculture and food industry mainly depend on freshwater use. The supply and demand gap for drinkable water rapidly increases each day and by the year 2030, it is predicted to reach 40% gaps [1].

Desalination is the most widely used method for producing fresh water. All desalination methods require energy input to produce fresh water from salty water. Although initial and operation costs of the desalination systems change according to the type and scale of the preferred system, the source of energy used directly affects the cost of the desalination system as well as its environmental effects. One of the best ways to decrease the costs and environmental effects is to use renewable energy sources to operate desalination systems.

Solar-powered desalination systems have a longer service life with few numbers of moving parts and low maintenance needs. They can be installed at remote places with poor or no infrastructure or energy grid [2].

Studies on solar-powered desalination systems mainly focus on increasing evaporation and condensation rates, recovering latent heat of condensation, and increasing productivity and system efficiency [3-6].

Enhancement of the distillate yield of the single-slope solar stills remains a popular area of study for many researchers. Some researchers used thermoelectric devices to boost solar still productivity. Esfahani et al. [7] fabricated and tested a new type of portable thermoelectric solar still. They used thermoelectric cooling technology to increase distillate water output. They found that the maximum efficiency during winter days was 13% and the average amount of daily output was 1.2 L/m^2. Rahbar et al. [8] carried out an experiment to investigate how a thermoelectric cooler influenced the rate of condensation in the portable solar still. They stated that during the experiment period, the portable solar still had a maximum daily efficiency of 7%. Rahbar et al. [9] carried out an experimental analysis of utilizing the thermoelectric cooler in solar still on the distillation performance in their designs. They compared water production from the thermoelectric cooling surface and the glass cover surface. They reported that the studied solar still has a minimum and maximum daily water productivities approximately 225 and 500 ml respectively. Al-Nimr et al. [10] proposed a novel hybrid desalination system that consists of a

* Corresponding author at: Kastamonu University, Mechanical Engineering Department, 37100 Kastamonu, Türkiye.

E-mail addresses: yozcan@kastamonu.edu.tr (Y. Özcan), edeniz@karabuk.edu.tr (E. Deniz).

Peer review under responsibility of Karabuk University.

https://doi.org/10.1016/j.jestch.2023.101362
2215-0986/

PV module, upper porous layer, air gap, lower porous layer, and thermoelectric cooler layer. They reported that the system produced 4.2 kg of water per day and had a 57.9% total efficiency. Nazari et al. [11] investigated the effect of the copper oxide (CuO_2) nanoparticles on the increased amount of evaporation and a utilizing cooling channel with the thermoelectric for cooling the glass cover to improve the condensation rate. Based on their results, the system's energy and exergy efficiencies were maximum enhanced by 80.6%, and 112.5% respectively, in comparison to the conventional ones. Dehghan et al. [12] employed a thermoelectric cooler to increase the temperature differential between the condensing and evaporating zones in their modelling solar still. This new type of thermoelectric-assisted solar still was mathematically modelled. They reported that the maximum value of energy and exergy efficiencies of the thermoelectric assisted solar still were about 55.1% and 2.9%, respectively. Rahbar et al. [13] experimentally investigated the effect of thermoelectric heating on solar desalination performance. They installed four thermoelectric modules at the bottom to warm the basin water. They reported that the maximum solar still exergy efficiency of utilizing thermoelectric heating was around 25%. Al-Madhhachi and Min [14] experimentally investigated a water distillation system incorporating the thermoelectric module. They investigate the influence of thermoelectric input energy, evaporation temperature, and vapor volume on the rate of freshwater output. According to their result, the water temperature has a major effect on the productivity of distillate water.

The disadvantage of thermoelectric cooling-heating systems is that they require energy to make a temperature difference. Based on the Seebeck effect, a TEG directly converts a temperature gradient into an electric voltage. So far, electricity could be generated from the difference in temperature between the condensate side inside the solar still and the atmospheric air side by using the thermoelectric module. Pradip et al. [15] investigated evacuated tubes coupled with solar stills (ETSC) and thermoelectric modules to increase performance. They concluded that the proposed combined TEG and ETSC system was capable of producing electrical energy and heating the water simultaneously for remote area applications and residential, with zero emissions. Shafii et al. [16] experimentally studied the effect of using TEG and evacuated tube solar collectors on desalination performance. They used a propeller fan to increase convection in the solar still to increase the condensation of water vapor. According to their results, the peak quantity of freshwater production was approximately 1110 $g/m^2.h$ and the improved solar desalination system's energy efficiency was 68%.

Changes in productivity amounts, energy and exergy efficiency in studies on similar systems are given in Table 1.

Aberuee et al. [27] demonstrated a solar desalination system with thermoelectric modules. The system was capable of producing electricity, fresh water, and warm water at the same time. They stated that the suggested system generated 896 kJ of electrical energy, 177 kg of fresh water, and 29 tons of hot water from 960 MJ/day of solar energy. Al-Nimr et al. [28] used TEG in the bottom of the basin, a PV cell module inside the still, and a finned condensation chamber to boost the pure water produced by the solar still. The TEG was installed under the basin to generate electricity by using the waste heat from the salty water. They indicated that the system's water output and electricity generations were 8.73 kg/day and 114.45 W, respectively, at 35 °C surrounding temperature, 1000 W/m^2 solar radiation intensity, and 5 m/s wind speed. Shoeibi et al. [29] experimentally investigated the effect of using thermoelectric cooling for reducing top glass cover temperature and thermoelectric heating for increasing the basin water temperature simultaneously on the distilled water production of solar desalination. They reported that solar desalination with thermoelectric modules and air fans enhanced freshwater output, thermal efficiency, and exergy efficiency by 79.4%, 11.2%, and 45.7%, respectively.

In this study, novel use of thermoelectric technology is used in solar desalination systems. Condensation latent heat is used to generate electricity via a thermoelectric module which is used to power a fan motor in order to increase the evaporation rate by forced convection. This new design with thermoelectric modules and fans has been tested under real conditions and proved to recover some waste heat and increased desalination yield. Energy-exergy analyses along with economic and enviro-economic analyses were conducted based on the system parameters and measurements taken from the designed experimental setup.

2. Experimental setup and theoretical analysis of the system

2.1. Experimental setup and procedure

The experiments were conducted with two similar single slope basin type solar stills in Karabuk (longitude: 32°657E, latitude: 41°207 N). Two systems (Fig. 1), one is conventional solar still (CSS), and the other is equipped with a thermoelectric module (CSS-TEG), were tested for six clear days from May to July 2021 between 8:00 am and 8:00 pm. To design CSS-TEG, the condensation surface on the back wall of the solar still, which is the top 280 mm of the back wall was replaced with an aluminium plate (2 × 280 × 1000 mm). Then a total of 32 thermal modules (4 rows × 8 columns) were glued onto this plate using thermal paste. A second layer of thermal paste was applied onto the modules and 4 heat sinks in total were glued onto the modules to improve cooling performance. 8 modules under each one of the heat sinks are connected in parallel, and 4 groups of 8 modules are connected in series. The output of this circuit is wired to a DC fan motor.

Thermoelectric modules in the experimental setup were employed to recover some amount of the latent heat that was lost during the condensation process. The thermoelectric generators use the temperature differential to generate electricity with the Seeback effect. Using a thermoelectric generator (TEG) some amount of energy from vapor condensation was recovered and converted to electrical energy, which was used to power fans placed near the water surface inside the solar still to accelerate the evaporation rate by forced convection. The novelty of this study is using TEG-powered fans inside the solar still to improve the evaporation rate by forced convection.

Technical specifications of the system components and design parameters are given in Table 2. The systems were inclined 35° south to enhance the quantity of solar energy hitting the surface aperture [30]. The condensed water on the glass surfaces of the distillation system was collected in the channels with a 5° slope and stored in the distilled water tank.

For all experiments, the basin's water level was 5 cm, and the total water volume in the basin was 50L. Saltwater samples were obtained from the Black Sea. Prior to doing any experimental measures, the experiment was carefully organized, with water supplied to the basin and the water level was set correctly. The amount of freshwater collected was carefully measured and recorded. After completing the daily experiment, the solar still system was prepared for the next measurement day.

The synchronization of the two solar stills (before modifications) was tested to prove that the two systems are identical before converting one of these stills to CSS-TEG. The two stills had the same volume of water in the basin and their production rate, basin, and water and glass temperatures were obtained for two days, and the results show that the two solar stills were in good synchrony before modification. After this synchronous test procedure, one of

Table 1
Comparison between the productivity and efficiency (Single slope solar still).

Modifications	Daily Productivity	Productivity Improvement	Energy Efficiency	Exergy Efficiency	Ref
Water depth 1 cm	1.485 kg	–	30.96%	3.48%	[17]
Water depth 2.5 cm	0.92 kg	-	19.21%	1.81%	
Conventional	2.940 L/m^2	-	–	–	[18]
Using water sprinkler	3.541 L/m^2	20%	-	-	
Conventional	–	-	36.7%	–	[19]
Propeller inside basin	-	17%	39.8%	-	
Conventional	0.595 kg	-	27.17%	–	[20]
Using agitation effect	0.830 kg	39.49%	30.57%	-	
Conventional	3.357 kg/m^2	-	32.9%	–	[21]
Paraffin wax in basin	3.762 kg/m^2	11.7%	37.10%	-	
Conventional	520 cc	-	–	–	[22]
Blades in the basin	545 cc	4.8%	-	-	
Conventional	3.2 L/m^2		18.16%	4.28%	[23]
Multi-wick solar still	4.22 L/m^2	31%	26.89%	5.31%	
Conventional	1.873 L/m^2	-	-	-	[24]
With vertical fins	2.322 L/m^2	24.19%	-	-	
With inclined fins	2.375 L/m^2	26.77%	-	-	
Conventional	3.75 kg/m^2	-	24.93%	1.69%	[25]
Using fins in basin	5.08 kg/m^2	35%	32%	2.81%	
Conventional	4.539 L/m^2	-	44.09%	–	[2]
Using fin in condenser	4.705 L/m^2	5%	45.70%	-	
Conventional	2.15 kg/m^2	-	22.7%	2.4%	[26]
Circular magnet in basin	2.82 kg/m^2	23.7%	23.2%	2.8%	
Rectangular magnet in basin	3.15 kg/m^2	31.7%	24.4%	2.9%	

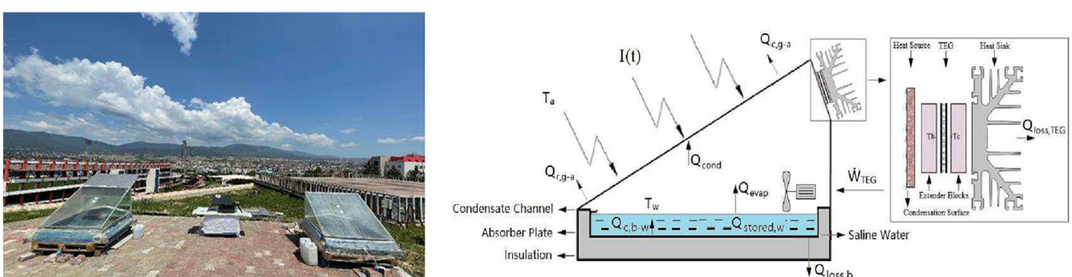

Fig. 1. Experimental setup of the CSS and CSS-TEG.

Table 2
Technical specifications of the solar still.

Specification	Dimensions	Specification	Dimensions
Glass cover area (m^2)	1.18	Basin tank dimensions (galvanized) (cm)	100*100
Glass thickness (mm)	4	Height of still from the ground (m)	0.20
East-West Side glass area (m^2)	0.34	SP1848 Thermoelectric Modul (mmxmm)	40x40
Height of basin, (m)	0.22(lower height)0.90 (higher height)	DC fan motor	1.2 V and 0.4A
The slope of glass (°)	35	Propeller dimension (mm)	21

the CSS was converted to CSS-TEG, and experiments were carried out.

The range and accuracy of the measurement equipment used in the study are illustrated in Table 3. The temperature of ambient air, glass cover, water, water vapor, basin, and thermoelectric module surfaces were measured using calibrated K-type thermocouples linked to a data module (Advantech Adam 4019+). A Solar 3120-type pyranometer was used to measure the solar radiation on the system's surface. At the same frequency, wind speed and distilled water output were measured using a portable anemometer and a graduated cylinder, respectively.

Table 3
Technical description of measurement devices.

Measurement devices	Range	Accuracy (±)
Data acquisition system (Adam 4019 +)	–	
Pyranometer (3120)	0–2000 W/m^2	±3% W/m^2
Anemometer (Testo 435)	0–20 m/s	±4% m/s
Thermocouple (K type)	0–200 °C	±0.1 °C
Measuring jar	0–500 ml	±5 ml

2.2. Theoretical analysis of solar distillation system

Compared to other designs, the single basin solar still is the least expensive and easy to fabricate [31]. Basin-type solar stills analysis will be simpler to understand, and the concepts developed from the investigations can be adapted to other designs.

2.2.1. System performance

Solar still works simply by allowing sun radiation to reach the bottom surface, where it is heated and water evaporation begins via heat transfer. There are several variables used to evaluate the thermal performance of the solar still system in terms of the amount of freshwater produced per unit of energy spent.

Hourly solar still efficiency is determined by the freshwater distillate by multiplying the latent heat of evaporation and dividing by the quantity of incoming solar radiation gathered at the same time interval. The following equation has been used to determine the performance of a solar still system which also means the instantaneous thermal efficiency of the solar stills during the experiment time [23,32].

$$\eta_i = \frac{\sum_{t=1}^{t=ET} \dot{m}_{ew} * h_{fg}}{\sum_{t=1}^{t=ET} I(t) * A_s * 3600s.h^{-1}} \quad (1)$$

The latent heat of evaporation was calculated [31] by;

$$h_{fg} = 2.4935 * 10^6 * (1 - 9.4779 * 10^{-4} * T_w + 1.3132 * 10^{-7} * T_w^2 - 4.7974 * 10^{-9} * T_w^3) \rightarrow T_w \leqslant 70 \quad (2)$$

where m_{ew} is the accumulated freshwater (kg/h), h_{fg} is the latent heat of evaporation (kJ/kg), I(t) is total solar intensity (W/m^2), A_s is the effective solar energy receiving area (m^2),T_w is the water temperature in the basin and ET is the experiment time. It is necessary to calculate the intensity of solar radiation on each wall.

$$I(t)_T = A_e \times I(t)_e + A_w \times I(t)_w + A_g \times I(t)_g \quad (3)$$

The solar radiation on any tilted surface can be conservatively calculated using the isotropic diffuse model [32]. The top glass cover allowed the most solar radiation into the solar still, emphasizing the importance of the top glass cover in delivering thermal energy for the evaporation process. The improvement might be attributed to taking configuration parameters into consideration when radiation transfers are calculated more precisely.

The daily energy efficiency for CSS and CSS-TEG was determined after the experimental work. To calculate the overall thermal efficiency of both stills, equation (4) was employed [20,33].

$$\eta = \frac{\sum \dot{m}_{ew} * h_{fg}}{\sum I(t) * A_s * 3600s.h^{-1}} \quad (4)$$

Also solar still with thermoelectric generators efficiency is defined [34];

$$\eta = \frac{\sum \dot{m}_{ew} * h_{fg} + P_{TEG}}{\sum I(t) * A_s * 3600s.h^{-1}} \quad (5)$$

In the previous equation, P_{TEG} indicates the energy generated at the system's output that is not utilized within the system. If generated electricity was used to run a fan, air pump, or other equipment within the solar still to boost the water output, the thermal efficiency could be determined the same as the conventional one.

2.2.2. Exergy analysis

Energy efficiency provides a quantitative assessment of how much energy is successfully used in the desalination process. Understanding all aspects of energy utilization in processes requires more than energy analysis. So exergy analysis must be performed on every thermal system in order to have an efficient design. Exergy analysis, as compared to energy analysis, provides a better understanding of how closely overall performance approaches ideal. An increase in irreversibility raises entropy generation while lowering system exergy efficiency. Therefore, all components of the equipment must have less irreversibility [35]. Exergy is a unit of measurement for energy quality that is described as the highest amount of useful work that may be accomplished as a system approaches equilibrium with a reference environment [36].

The solar still exergy efficiency could be defined as the ratio between the exergy of the product to the exergy input of solar radiation [31].

$$\eta_{Ex} = \frac{\dot{E}xproduct}{\dot{E}xin} \quad (6)$$

In reality, part of the evaporated water drop into the basin after condensation on the cover, therefore the calculated exergy production from the experimental data could be lower than the calculated values. Exergy product in a solar still is the result of evaporation of saline water and condensation of vapor. Hourly the solar still exergy output can be found as [37];

$$\dot{E}xproduct = \frac{\dot{m}_{ew} * h_{fg}}{\left(3600s.h^{-1}\right)}\left[1 - \frac{(T_a + 273)}{(T_w + 273)}\right] \quad (7)$$

where is the hourly distillate water (kg/h), h_{fg} is the latent heat of evaporation (J/kg), T_a is the ambient air temperature (°C) and T_w is the basin water temperature (°C).

The solar still utilized in the study distills saltwater using solar energy obtained on the surface of the still, and the exergy input of this system can be expressed as;

$$\dot{E}x_{in} = \dot{m}_{sw}Ex_{sw} + \dot{E}x_{sun}(SS) \quad (8)$$

The exergy is lost because of the heat loss from the solar still to the outside. Assuming the seawater is at a thermodynamic dead state ($m_{sw}Ex_{sw} = 0$) the exergetic efficiency or second law efficiency can be found as;

$$\eta_{Ex} = \frac{\dot{m}ew \times \dot{E}x_{ew}}{\dot{E}x_{sun}} \quad (9)$$

For CSS-TEG, since the required energy for the fan is provided by TEG from the condensation process, the exergy input of CSS and new type solar still are only the exergy of the solar irradiation (E_{Xsun}). The solar still's exergy is derived by multiplying the incoming solar radiation by the Petela expression [38];

$$\dot{E}x_{sun}(SS) = I(t)_T * \left[1 - \frac{4}{3}\left(\frac{T_a + 273}{T_{sun}}\right) + \frac{1}{3}\left(\frac{T_a + 273}{T_{sun}}\right)^4\right] \quad (10)$$

where $I\ (t)_T$ is total solar irradiation on the glass cover of the solar still (W/m^2) and T_s is the solar radiation temperature 6000 K, and, the above equation can be simplified as;

$$\dot{E}x_{in}(SS) = I(t)_T * 0.933 \quad (11)$$

Exergy efficiency of the solar still;

$$\eta_{Ex} = \frac{\frac{\dot{m}_{ew}}{(3600s.h^{-1})} h_{fg}\left[1 - \frac{(T_a+273)}{(T_w+273)}\right]}{I(t)_T \times \left[1 - \frac{4}{3}\left(\frac{T_a+273}{T_{sun}}\right) + \frac{1}{3}\left(\frac{T_a+273}{T_{sun}}\right)^4\right]} \quad (12)$$

2.2.3. Economic and enviro-economic analyses

Economic analysis is used in desalination systems to assess the cost of 1 L of distillate water. Furthermore, enviro-economic analysis is a policy strategy that encourages the use of renewable energy to minimize carbon emissions. The capital costs of a solar still have an impact on the cost of producing water and the system's exergoeconomic outcomes. Aside from capital price (P), capital recovery factor (CRF), fixed annual cost (FAC), annual salvage value (ASV), annual maintenance cost (AMC), average annual water production (M), annual cost (AC), and sinking fund factor (SFF) must be considered as the primary variables in a detailed economic analysis of solar desalination units [7].

In this regard, the capital recovery factor (CRF) can be determined as [39];

$$CRF = \frac{i(1+i)^n}{(1+i)^n - 1} \quad (13)$$

where, i is the interest rate (10% in Türkiye) and n represent the projected operational life of the system which is considered 20 years.

The first annual cost of solar desalination (FAC) becomes;

$$FAC = P \times CRF \quad (14)$$

Capital cost (P) can be estimated by adding the costs of utilized materials such as galvanized steel sheet, glass cover, spray paint, TEG, heat sink, DC fan, etc. as well as labor costs.

In this study, the capital cost (P) is equal to 150 $ for the traditional unit and 250 $ for the new type of solar still (100$ for the heat sink, and 32-piece TEG and 2 fans). By assuming that the system salvage value (S) is equal to 20% of the capital price and the sinking fund factor (SFF) and annual salvage value (ASV) is obtained [7];

$$SFF = \frac{i}{(1+i)^n - 1} \quad (15)$$

$$ASV = SFF \times S \quad (16)$$

Annual maintenance cost (AMC) of the system includes; gathering fresh water, wiping the glass cover, and DC fan maintenance. AMC is estimated to be 15% of the FAC in this case;

$$AMC = 0.15 \times FAC \quad (17)$$

As a result, the annual cost (AC) of the solar still system is obtained by;

$$AC = FAC + AMC - ASV \quad (18)$$

Eventually, the pricing of distilled water per liter (CPL) could be estimated as follows;

$$CPL = \frac{AC}{M} \quad (19)$$

where M is the annual water production per square meter of the solar desalination system.

A solar still payback time is calculated using the following equation [34,40];

$$P_B = \frac{In\left[\frac{M \times S_p}{(M \times S_p) - (P \times i)}\right]}{In(1+i)} \quad (20)$$

where Sp is the selling price of distillate water.

The enviro-economic analysis is part of economic analysis that focuses on environmental issues. Its goal is to determine the system's performance in using renewable energy sources and reducing CO_2 emissions into the environment. The enviro-economic analysis is carried out by calculating the cost of carbon emissions, which is nearly 0.96 kg per kWh of electricity. Moreover, due to transmission and distribution losses caused by inefficient equipment, the CO_2 output per kWh is equal to 2 kg. The CO_2 mitigation from the solar desalination system considering the energy and exergy approach is given by [29,41];

$$\Phi_{En}CO_2 = (E_{product} \times n) \times \psi \quad (21)$$

$$\Phi_{Ex}CO_2 = (Ex_{out} \times n) \times \psi \quad (22)$$

where ψ is the CO_2 emission (2 kg CO_2/kWh) caused by the use of coal to generate electricity and Exout is the exergy output from the solar distiller per annum. For the high and low commitment scenarios, the international carbon price (z_{CO2}) is between 16 $/tCO_2$ and 13 $/tCO_2$. As a result, for the enviro-economic study, the mean value of 14.5 $/tCO_2$ is used [42]. The environmental cost (Z_{CO2}) is calculated using the provided equation by Rajoria et al. [42];

$$Z_{En}CO_2 = z_{CO_2} \times \Phi_{CO_2} \quad (23)$$

$$Z_{Ex}CO_2 = z_{CO_2} \times \Phi_{Ex}CO_2 \quad (24)$$

2.2.4. Error analysis

In experimental measurements, uncertainty is split into two categories: random errors and systematic errors. The present study presumes that the data measurements are uniformly distributed, so systematic error is used for uncertainty analysis [8]. Kline and McClintock [43] proposed an equation for calculating the uncertainty of experimental data.

$$w_r = \left[\left(\frac{\partial R}{\partial x_1} w_1\right)^2 + \dots + \left(\frac{\partial R}{\partial x_i} w_i\right)^2\right]^{1/2} \quad (25)$$

where x represents the independent variable, R represents the function and w_r represents the total uncertainty. By substituting the energy efficiency into the Eq. (25), the uncertainty of energy efficiency can be determined by [8];

$$w(\eta_{energy}) = \left[\left(\frac{\partial \eta_{energy}}{\partial m_w} \times w_{m_w}\right)^2 + \left(\frac{\partial \eta_{energy}}{\partial h_{fg}} \times w_{h_{fg}}\right)^2 + \left(\frac{\partial \eta_{energy}}{\partial I(t)} \times w_{I(t)}\right)^2\right]^{1/2} \quad (26)$$

$$w(\eta_{energy}) = \eta_{energy} \times \left[\frac{(w_{m_w})^2}{m_w^2} + \frac{(w_{h_{fg}})^2}{h_{fg}^2} + \frac{(w_{I(t)})^2}{I(t)^2}\right]^{1/2} \quad (27)$$

Using the above-mentioned equations, the uncertainty in daily energy efficiency is predicted to be roughly 0,24%.

3. Results and discussion

The energy, exergy, economic and enviro-economic (4E) behaviors of a CSS-TEG were studied experimentally under real environmental conditions. There is no study in the literature that gives an analysis of a CSS-TEG using an air circulating fan unit, including 4E analyses. The experimental study was carried out over several days

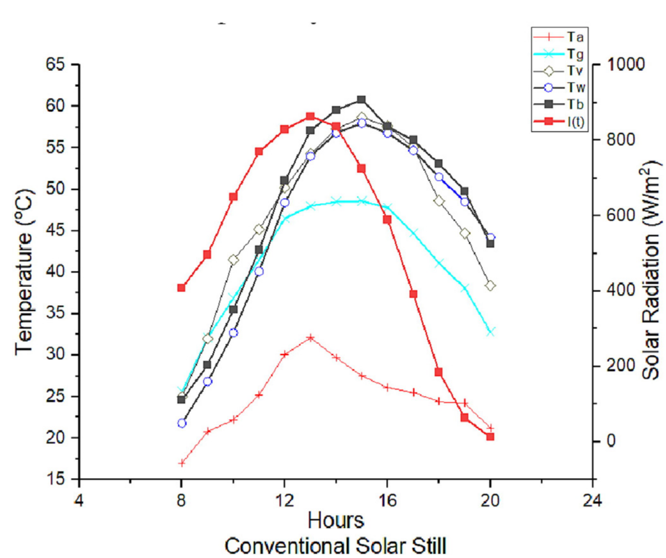

Fig. 2. Hourly measured temperatures and solar radiation CSS.

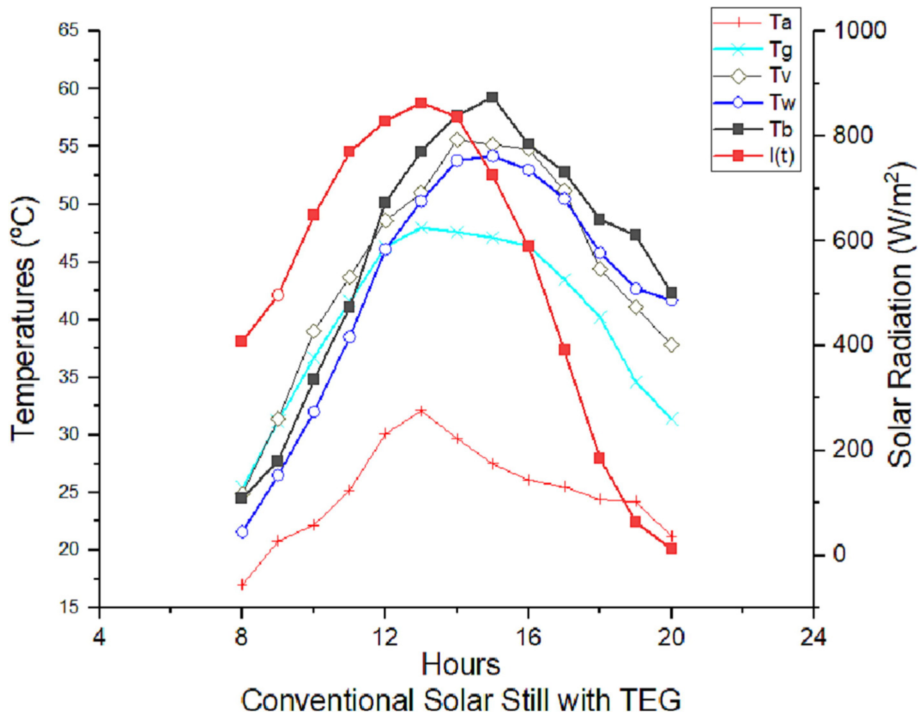

Fig. 3. Hourly measured temperatures and solar radiation CSS-TEG.

during the 2021 summer. The studies were performed at 5 cm water depth in the still basin. Figs. 2 and 3 demonstrate the variation of solar radiation and the measured temperatures during the experiment. The highest solar intensity reached 864 W/m^2 around 13:00 and the maximum ambient temperature was 32,1 °C.

Fig. 3 clearly show that the TEG and fan system had a considerable influence on the still temperatures. The water and glass temperature in CSS-TEG were lower compared to that of CSS. The maximum Tw and Tg observed with CSS-TEG were 54.2 °C and 48 °C respectively, whereas, with CSS, they were 58°C and 48.6°C, respectively.

Fig. 4 shows that the difference in temperature between the TEG's hot and cold sides was low in the morning, then increases by the solar irradiance, and decreases in the afternoon as the solar radiation weakens. When the temperature difference between the cold side and the hot side increases, the TEG begins to produce enough voltage to run fans. The fans started running after 11 am and operated until 5 pm because of the temperature difference

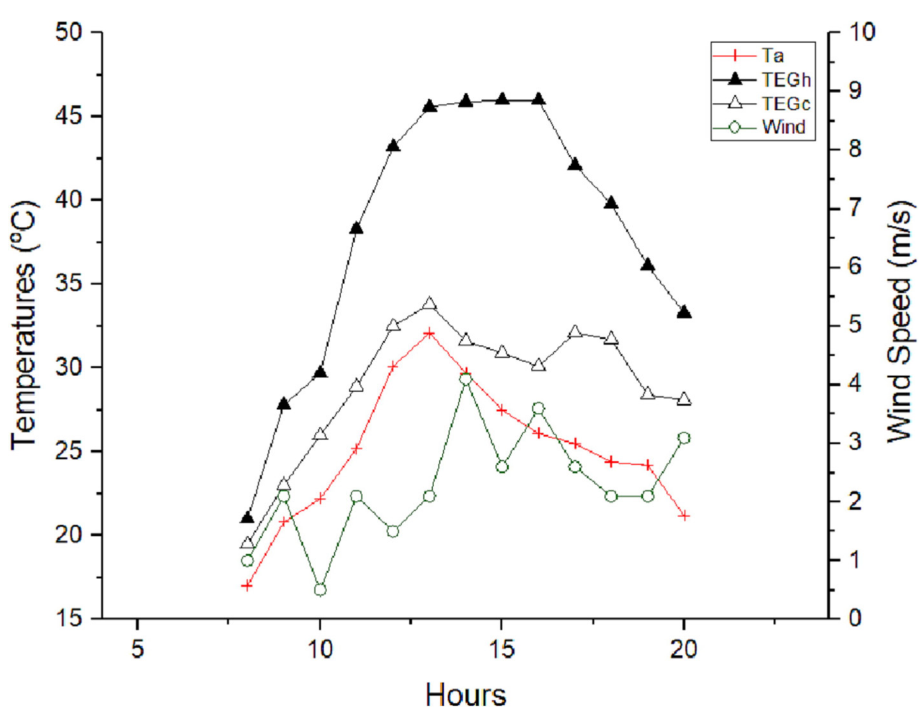

Fig. 4. Hourly wind speed, the ambient and TEG surface temperatures.

between TEG surfaces. The highest temperature difference among the module surfaces was recorded at 15.9 °C around 2:00 pm, and maximum electricity was generated by TEGs. Fans increase the evaporation rate by introducing forced convection mechanism into the still. Continuous circulation of the air over the water surface reduces the relative humidity near contact surface and creates negative partial pressure hence increasing the rate of evaporation and the quantity of freshwater distilled.

As seen in Fig. 5 the amount of output water was low in the morning because solar radiation and ambient temperatures were low. The hourly production of the stills reached their peak values at 17:00. The daily average distillate production rates of CSS and CSS-TEG were 3263, 3853 g/m^2 during the day and 1060, 1040 g/m^2 during the night, respectively. The daily productivity of the CSS-TEG increased by 13.44% relative to the CSS.

Fig. 6 and Fig. 7 show hourly variations of energy and exergy efficiency for CSS-TEG and CSS. The results demonstrate that the energy efficiencies for both solar stills began by zero at 8:00 since there was no production at the start of the experiment and instantaneous efficiencies slowly increased with time. The quantity of solar irradiance falling on the system diminishes near the time of sunset, however, the distillation process continues because of stored the energy in the system. As a result of this, the highest hourly energy and exergy efficiencies are seen during this period. On the basis of daily energy and exergy efficiency, the CSS-TEG has outperformed in comparison to the CSS. The daily energy and exergy efficiencies calculated for CSS-TEG were 40.34% and 2.462% respectively, whereas, for CSS, they were 35.55% and 2.403%, respectively.

In desalination plants, the economic analysis of the system is a key indicator of the acceptability of the model. Table 4 gives the cost analysis of the solar still. The primary goal of the manufacturing process and operation costs to keep as low as possible. The enviro-economic analysis finds solutions for lowering the environmental effect associated with the whole system.

It should be noted that to calculate annual production and the annual exergy outputs, the daily average the exergy outputs and productivity of the experimented day multiplied by the number of clear days throughout the year [44]. Karabuk city has 82.9 clear days in a year [37]. The yearly exergy outputs have been calculated as 14.97 kWh for CSS, and 15.33 kWh for CSS-TEG. The exergoeconomic parameters for CSS and CSS-TEG were 0.43 kWh/$ and 0.44 kWh/$ respectively. Referring to the exergo-environmental parameter, CSS and CSS-TEG mitigated on average 0.596 and 0.6132 tonnes of CO_2 respectively. The unique solar still reduced CO_2 emissions more than the conventional still because of its greater exergy outputs during its lifespan.

4. Conclusions and recommendations

The effects of utilizing TEG used to power a fan motor in the conventional single slope solar still are experimentally investigated. The aim of this study was to determine the effect of TEG system on the still's performance. The water productivity, energy and exergy efficiency of two solar stills are compared. An economic analysis is performed to evaluate the overall cost of the system as well as the payback period.

Some of the significant conclusions of this work are below:

- As for the studies presented in Table 1, it can be seen that the improvement in productivity, energy and exergy efficiency values range from 5 to 40%, 18 to 45%, and 1.69 to 5.31% respectively.
- The highest productivity time period of solar still is from 1:00 pm to 5:00 pm.
- The average daily productivity of CSS and CSS-TEG were 4313 g/m^2 and 4893 g/m^2 respectively.
- The unit productivity increases with air circulation in the solar still.
- The variations in hourly energy and exergy efficiency follow a similar pattern.
- The daily energy and exergy efficiency of CSS-TEG are about 40.34% and 2.462% respectively, whereas, with CSS, they are 35.55% and 2.403%, respectively.
- Estimated cost of distillate water by CSS and CSS-TEG systems are 0.055 and 0.081 US$/kg respectively.
- The environmental cost of CSS and CSS-TEG systems, also known as the enviro-economic parameter, is calculated to be 0.0298 and 0.03066 ton of CO_2 reduction per year and is estimated to be 8.642 and 8.8914$ respectively for 20 year service life.

Further studies may include and focus on the following subjects

- Using an air bubbling device instead of circulation fan to increase water evaporation.

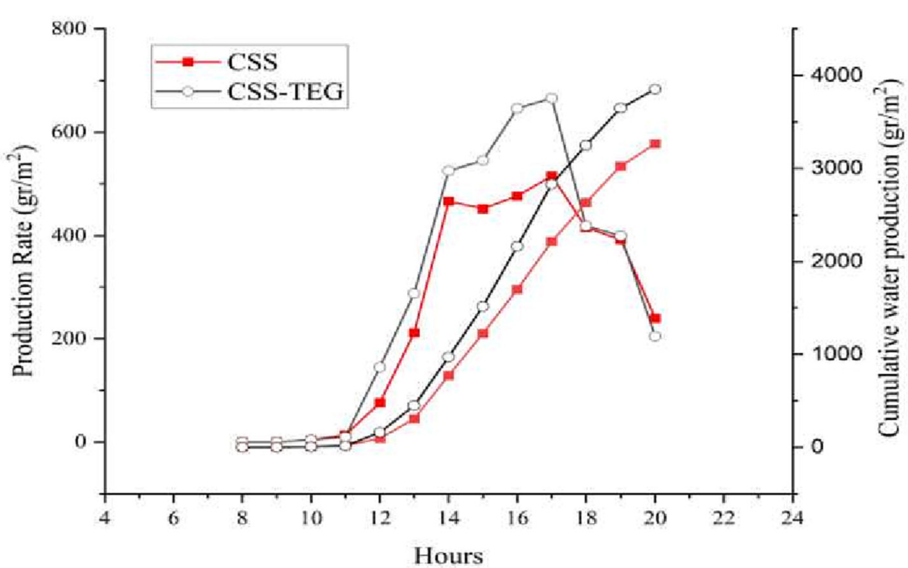

Fig. 5. Hourly and cumulative water productivity of CSS and CSS-TEG.

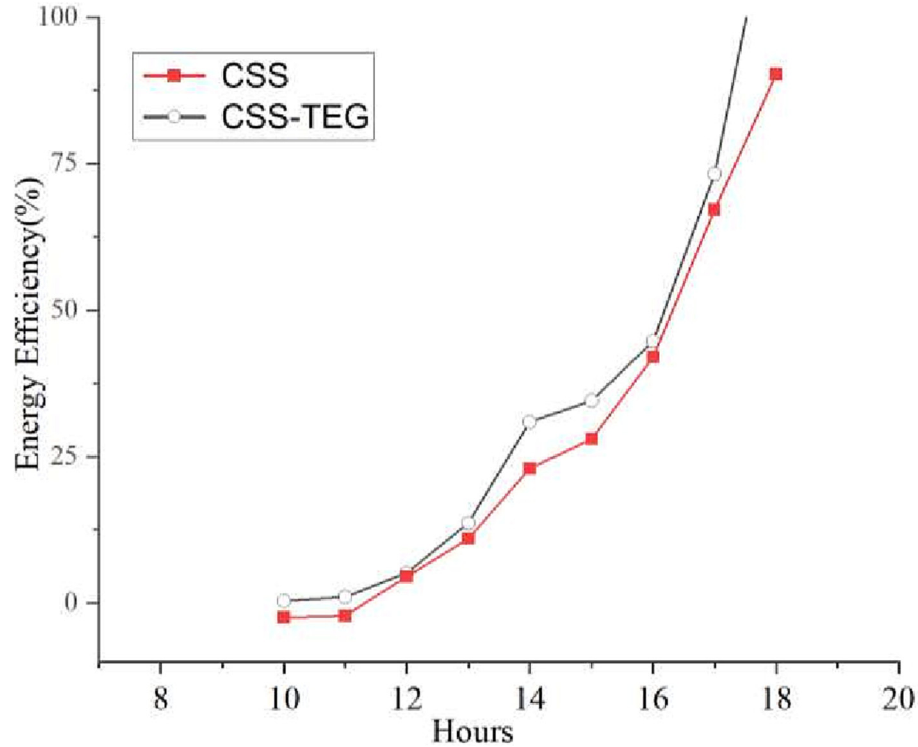

Fig. 6. The hourly energy efficiency of the CSS-TEG and CSS.

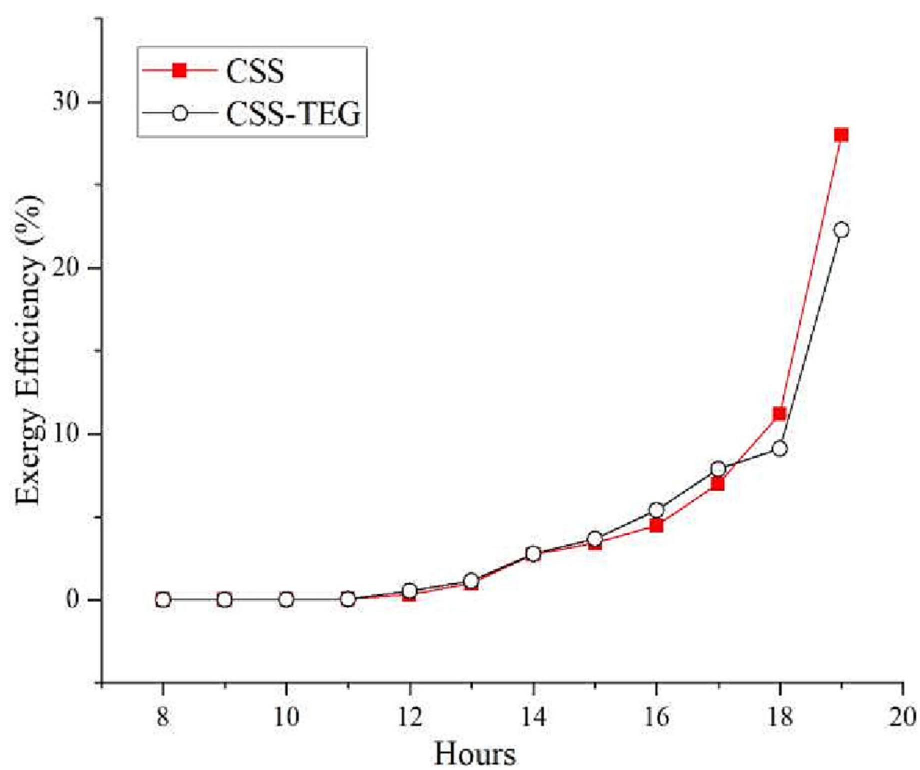

Fig. 7. The hourly exergy efficiency of the CSS-TEG and CSS.

- Using an air bubbling and air circulation together to improve water productivity.
- The temperature difference between the thermoelectric hot and cold surface can be increased. The module's cold side can be redesigned to come into contact with the cold water running system.
- TEG can be used on conventional desalination systems with passive condenser to increase system productivity.

Table 4
The results of cost analysis for the study.

Parameter	CSS	CSS-TEG	Unit
M	357.5	405.6	kg/m^2
i	10		
n	20		
CRF	0.117	0.117	
P	150	250	$
FAC	17.61	29.3	$
S	30	50	$
SFF	0.017	0.017	
ASV	0.52	0.872	$
AMC	2.64	4.404	$
AC	19.73	32.89	$
CPL	0.055	0.081	$\$/kg/m^2$
Z_{ExCO2}	8.642	8.891	$

Declaration of Competing Interest

The authors declare that they have no known competing financial interests or personal relationships that could have appeared to influence the work reported in this paper.

References

[1] A. Boretti, L. Rosa, Reassessing the projections of the World Water Development Report, n.d. https://www.nature.com/articles/s41545-019-0039-9.

[2] H.S. Mohaisen, J.A. Esfahani, M.B. Ayani, Improvement in the performance and cost of passive solar stills using a finned-wall/built-in condenser: An experimental study, Renew. Energy 168 (2021) 170–180, https://doi.org/10.1016/j.renene.2020.12.056.

[3] M.K. Phadatare, S.K. Verma, Influence of water depth on internal heat and mass transfer in a plastic solar still, Desalination 217 (2007) 267–275, https://doi.org/10.1016/j.desal.2007.03.006.

[4] K. Kalidasa Murugavel, K.K.S.K. Chockalingam, K. Srithar, Progresses in improving the effectiveness of the single basin passive solar still, Desalination 220 (1–3) (2008) 677–686, https://doi.org/10.1016/j.desal.2007.01.062.

[5] V.K. Dwivedi, G.N. Tiwari, Comparison of internal heat transfer coefficients in passive solar stills by different thermal models: An experimental validation, Desalination. 246 (2009) 304–318, https://doi.org/10.1016/j.desal.2008.06.024.

[6] R. Sathyamurthy, S.A. El-Agouz, P.K. Nagarajan, J. Subramani, T. Arunkumar, D. Mageshbabu, B. Madhu, R. Bharathwaaj, N. Prakash, A Review of integrating solar collectors to solar still, Renew. Sustain. Energy Rev. 77 (2017) 1069–1097, https://doi.org/10.1016/j.rser.2016.11.223.

[7] J.A. Esfahani, N. Rahbar, M. Lavvaf, Utilization of thermoelectric cooling in a portable active solar still — An experimental study on winter days, Desalination. 269 (2011) 198–205, https://doi.org/10.1016/j.desal.2010.10.062.

[8] N. Rahbar, J.A. Esfahani, Experimental study of a novel portable solar still by utilizing the heatpipe and thermoelectric module, Desalination. 284 (2012) 55–61, https://doi.org/10.1016/j.desal.2011.08.036.

[9] N. Rahbar, J.A. Esfahani, A. Asadi, An experimental investigation on productivity and performance of a new improved design portable asymmetrical solar still utilizing thermoelectric modules, Energy Convers. Manag. 118 (2016) 55–62, https://doi.org/10.1016/j.enconman.2016.03.052.

[10] M.A. Al-Nimr, W.A. Al-Ammari, A. Alkhalidi, A novel hybrid photovoltaics/thermoelectric cooler distillation system, Int. J. Energy Res. 43 (2019) 791–805, https://doi.org/10.1002/er.4309.

[11] S. Nazari, H. Safarzadeh, M. Bahiraei, Performance improvement of a single slope solar still by employing thermoelectric cooling channel and copper oxide nanofluid: An experimental study, J. Clean. Prod. 208 (2019) 1041–1052, https://doi.org/10.1016/j.jclepro.2018.10.194.

[12] A.A. Dehghan, A. Afshari, N. Rahbar, Thermal modeling and exergetic analysis of a thermoelectric assisted solar still, Sol. Energy. 115 (2015) 277–288, https://doi.org/10.1016/j.solener.2015.02.038.

[13] N. Rahbar, A. Gharaiian, S. Rashidi, Exergy and economic analysis for a double slope solar still equipped by thermoelectric heating modules - an experimental investigation, Desalination. 420 (2017) 106–113, https://doi.org/10.1016/j.desal.2017.07.005.

[14] H. Al-Madhhachi, G. Min, Key factors affecting the water production in a thermoelectric distillation system, Energy Convers. Manag. 165 (2018) 459–464, https://doi.org/10.1016/j.enconman.2018.03.080.

[15] H. Pradeep, S. Sharin, Hybrid solar still with thermoelectric generators and evacuated tubes, Int. J. Ignited Minds. (2015) 49–59.

[16] M.B. Shafii, M. Shahmohamadi, M. Faegh, H. Sadrhosseini, Examination of a novel solar still equipped with evacuated tube collectors and thermoelectric modules, Desalination. 382 (2016) 21–27, https://doi.org/10.1016/j.desal.2015.12.019.

[17] S. Vaithilingam, G.S. Esakkimuthu, Energy and exergy analysis of single slope passive solar still: an experimental investigation, Desalin. Water Treat. 55 (2014) 1433–1444, https://doi.org/10.1080/19443994.2014.928794.

[18] B. Gupta, R. Sharma, P. Shankar, P. Baredar, Performance enhancement of modified solar still using water sprinkler: An experimental approach, Perspect. Sci. 8 (2016) 191–194, https://doi.org/10.1016/j.pisc.2016.04.029.

[19] Z.M. Omara, A.S. Abdullah, T. Dakrory, Improving the productivity of solar still by using water fan and wind turbine, Sol. Energy. 147 (2017) 181–188, https://doi.org/10.1016/j.solener.2017.03.041.

[20] R.A. Kumar, G. Esakkimuthu, K.K. Murugavel, Performance enhancement of a single basin single slope solar still using agitation effect and external condenser, Desalination. 399 (2016) 198–202, https://doi.org/10.1016/j.desal.2016.09.006.

[21] S.M. Shalaby, E. El-Bialy, A.A. El-Sebaii, An experimental investigation of a v-corrugated absorber single-basin solar still using PCM, Desalination. 398 (2016) 247–255, https://doi.org/10.1016/j.desal.2016.07.042.

[22] S. Rashidi, J. Abolfazli Esfahani, N. Rahbar, Partitioning of solar still for performance recovery: Experimental and numerical investigations with cost analysis, Sol. Energy. 153 (2017) 41–50, https://doi.org/10.1016/j.solener.2017.05.041.

[23] P. Pal, R. Dev, Thermal modeling, experimental validation, and comparative analysis of modified solar stills, J. Sol. Energy Eng. 141 (2019), https://doi.org/10.1115/1.4043955.

[24] H. Panchal, D. Mevada, K.K. Sadasivuni, F.A. Essa, S. Shanmugan, M. Khalid, Experimental and water quality analysis of solar stills with vertical and inclined fins, Groundw. Sustain. Dev. 11 (2020), https://doi.org/10.1016/j.gsd.2020.100410 100410.

[25] S. Vaithilingam, V. Muthu, M.M. Athikesavan, A. Afzal, R. Sathyamurthy, Energy and exergy analysis of conventional acrylic solar still with and without copper fins, Environ. Sci. Pollut. Res. 29 (2022) 6194–6204, https://doi.org/10.1007/s11356-021-16124-2.

[26] R. Dhivagar, S. El-Sapa, A.J. Alrubaie, A. Al-Khaykan, A.J. Chamkha, H. Panchal, M.S. El-Sebaey, K. Sharma, A case study on thermal performance analysis of a solar still basin employing ceramic magnets, Case Stud. Therm. Eng. 39 (2022), https://doi.org/10.1016/j.csite.2022.102402 102402.

[27] M.J. Aberuee, E. Baniasadi, M. Ziaei-Rad, Performance analysis of an integrated solar based thermo-electric and desalination system, Appl. Therm. Eng. 110 (2017) 399–411, https://doi.org/10.1016/j.applthermaleng.2016.08.199.

[28] M.A. Al-Nimr, K.S. Qananba, A solar hybrid system for power generation and water distillation, Sol. Energy. 171 (2018) 92–105, https://doi.org/10.1016/j.solener.2018.06.019.

[29] S. Shoeibi, N. Rahbar, A. Abedini Esfahlani, H. Kargarsharifabad, Energy matrices, economic and environmental analysis of thermoelectric solar desalination using cooling fan, J. Therm. Anal. Calorim. 147 (2022) 9645–9660, https://doi.org/10.1007/s10973-022-11217-7.

[30] S.K. Singh, S.C. Kaushik, V.V. Tyagi, S.K. Tyagi, Comparative Performance and parametric study of solar still: A review, Sustain. Energy Technol. Assessments. 47 (2021), https://doi.org/10.1016/j.seta.2021.101541 101541.

[31] S.W. Sharshir, A.H. Elsheikh, G. Peng, N. Yang, M.O.A. El-Samadony, A.E. Kabeel, Thermal performance and exergy analysis of solar stills – A review, Renew. Sustain. Energy Rev. 73 (2017) 521–544, https://doi.org/10.1016/j.rser.2017.01.156.

[32] M. Hedayatizadeh, F. Sarhaddi, Thermal simulation of a modified solar desalination system with four transparent apertures with the aim of productivity augmentation, Comput. Chem. Eng. 150 (2021), https://doi.org/10.1016/j.compchemeng.2021.107314 107314.

[33] C. Elango, N. Gunasekaran, K. Sampathkumar, Thermal models of solar still—A comprehensive review, Renew. Sustain. Energy Rev. 47 (2015) 856–911, https://doi.org/10.1016/j.rser.2015.03.054.

[34] A.W. Jeevadason, S. Padmini, C. Bharatiraja, A.E. Kabeel, A review on diverse combinations and Energy-Exergy-Economics (3E) of hybrid solar still desalination, Desalination. 527 (2022), https://doi.org/10.1016/j.desal.2022.115587 115587.

[35] H. Aghaei Zoori, F. Farshchi Tabrizi, F. Sarhaddi, F. Heshmatnezhad, Comparison between energy and exergy efficiencies in a weir type cascade solar still, Desalination. 325 (2013) 113–121, https://doi.org/10.1016/j.desal.2013.07.004.

[36] K.R. Ranjan, S.C. Kaushik, Energy, exergy and thermo-economic analysis of solar distillation systems: A review, Renew. Sustain. Energy Rev. 27 (2013) 709–723, https://doi.org/10.1016/j.rser.2013.07.025.

[37] E. Deniz, S. Çınar, Energy, exergy, economic and environmental (4E) analysis of a solar desalination system with humidification-dehumidification, Energy Convers. Manag. 126 (2016) 12–19, https://doi.org/10.1016/j.enconman.2016.07.064.

[38] A.G.M. Ibrahim, I. Dincer, A solar desalination system: Exergetic performance assessment, Energy Convers. Manag. 101 (2015) 379–392, https://doi.org/10.1016/j.enconman.2015.05.060.

[39] A. Kianifar, S. Zeinali Heris, O. Mahian, Exergy and economic analysis of a pyramid-shaped solar water purification system: Active and passive cases, Energy. 38 (2012) 31–36, https://doi.org/10.1016/j.energy.2011.12.046.

[40] O. Bait, Exergy, environ–economic and economic analyses of a tubular solar water heater assisted solar still, J. Clean. Prod. 212 (2019) 630–646, https://doi.org/10.1016/j.jclepro.2018.12.015.

[41] G.N. Tiwari, J.K. Yadav, D.B. Singh, I.M. Al-Helal, A.M. Abdel-Ghany, Exergoeconomic and enviroeconomic analyses of partially covered photovoltaic flat plate collector active solar distillation system, Desalination. 367 (2015) 186–196, https://doi.org/10.1016/j.desal.2015.04.010.
[42] C.S. Rajoria, S. Agrawal, G.N. Tiwari, Exergetic and enviroeconomic analysis of novel hybrid PVT array, Sol. Energy. 88 (2013) 110–119, https://doi.org/10.1016/j.solener.2012.11.018.
[43] M.C. Kline, S. J., Describing Uncertainties in Single-Sample Experiments, (1953).
[44] A.R.A. Elbar, M.S. Yousef, H. Hassan, Energy, exergy, exergoeconomic and enviroeconomic (4E) evaluation of a new integration of solar still with photovoltaic panel, J. Clean. Prod. 233 (2019) 665–680, https://doi.org/10.1016/j.jclepro.2019.06.111.